Journal of Solid State Chemistry **165,** 56–64 (2002)
doi:10.1006/jssc.2002.9493, available online at http://www/idealibrary.com on IDEAL®

Disordering and Electronic State of Cobalt Ions in Mechanochemically Synthesized $LiCoO_2$

N. V. Kosova,*[,1] V. F. Anufrienko,† T. V. Larina,† A. Rougier,‡ L. Aymard,‡ and J. M. Tarascon‡

*Institute of Solid State Chemistry, †Boreskov' Institute of Catalysis, Siberian Branch of Russian Academy of Sciences, 18 Kutateladze, Novosibirsk 630128, Russia; and ‡Laboratoire de Réactivité et Chimie des Solides, Université de Picardie Jules Verne, France
E-mail: kosava@solid.nsc.ru

Received August 7, 2001; in revised form November 19, 2001; accepted December 21, 2001

Mechanical activation (MA) combined with heat treatment at moderate temperatures was used to prepare disordered and highly dispersed $LiCoO_2$ starting from the mixtures of various cobalt precursors (CoOOH, $Co(OH)_2$, and Co) and LiOH. X-ray powder diffraction and IR spectroscopy were used to investigate the phase composition and the crystal structure of as-prepared samples, while the electronic state of cobalt ions was characterized by diffuse reflectance electron spectroscopy. MA of the LiOH + CoOOH mixture led to the formation of LT-$LiCoO_2$ with a cubic spinel-related structure. Heat treatment at 600°C of the latter resulted in the formation of HT-$LiCoO_2$ with a hexagonal layered structure similar to ceramic $LiCoO_2$. However, as-prepared HT-$LiCoO_2$ is characterized by $Co^{3+}O_6$ octahedra less perfect than those of ceramic $LiCoO_2$. All MA-$LiCoO_2$ samples are exclusively described by localized *d* electrons. © 2002 Elsevier Science (USA)

INTRODUCTION

$LiCoO_2$ is widely studied by numerous researchers as a promising positive electrode material for secondary lithium batteries (1–3). Over the past few years a great deal of attention has been devoted to the preparation of metastable lithium–transition metal oxides of unusual ordering (structural, magnetic, charge) and valence states of ions that cannot be obtained by conventional high-temperature techniques. The structure of such products, as expected, should be more stable to intercalation/deintercalation of lithium ions in the course of discharge/charge processes, thus, providing better electrochemical behavior and preventing structural distortion. Phase transition occurs when an electron density, arising from the inserted atoms, destabilizes vacant levels of the matrix, and a more effective electron stabilization of the system can be provided as a result of irreversible structural transition (4). For example, while cycling an $LiCoO_2$/Li electrochemical cell, $LiCoO_2$ exhibits a monoclinic distortion for $x = 0.5$, which was associated with an interslab Li/vacancy ordering (5). Thus, the need for cathode materials with suitable crystal and electronic structure that could provide intercalation/deintercalation without sharp structural distortion and, therefore, band destabilization is highlighted.

Structural disordering in $LiCoO_2$ can be achieved by cation or anion nonstoichiometry, cation mixing, and a disturbance of oxygen layers stacking. Generally, it corresponds to the weakening of *d*-ions correlation, resulting in the full localization of *d* electrons on the transition metals ions, as a limit (6). Low-temperature methods are usually used to prepare disordered $LiCoO_2$.

As reported in the literature, $LiCoO_2$ exhibits low- and high-temperature forms, depending on the synthesis temperature. HT-$LiCoO_2$ has a hexagonal structure, while LT-$LiCoO_2$ has a cubic structure. The hexagonal and cubic structures are based on the same oxygen sublattice, and are distinguished by the spatial arrangement of cations. HT-$LiCoO_2$ exhibits an ideal α-$NaFeO_2$ layered structure (S.G.: $R\bar{3}m$) with an ABCABC oxygen stacking (7). LT-$LiCoO_2$ is believed to adopt a spinel-related structure (S.G.:$Fd\bar{3}m$) based on a cubic closed packed oxygen network with alternating cation layers of 0.75 Co, 0.25 Li and 0.75 Li, 0.25 Co composition perpendicular to each of the four cubic (111) directions (1).

Rossen *et al.* obtained LT-$LiCoO_2$ by mixing $LiOH \cdot H_2O$ and $CoCO_3$ at 400°C in alumina boats under extra dry air for 90 h, with a final grinding (1). Sometimes, low-temperature methods were found to produce HT-$LiCoO_2$. In this case, cobalt hydroxides ($Co(OH)_2$ or CoOOH) were usually found to be more reactive precursors than Co_3O_4. The higher reactivity of these compounds in the synthesis of layered $LiCoO_2$ is most likely nested in the similarity of their structures ($R\bar{3}m$ for CoOOH and *P*-3-*m*1 for $Co(OH)_2$) and in their larger specific surface area. When interacting with LiOH,

[1]To whom correspondence should be addressed. Fax: 7-3832-322847.

0022-4596/02 $35.00

CoOOH and $Co(OH)_2$ exhibit their amphotheric properties. Chiang *et al.* prepared HT-$LiCoO_2$ by freeze-drying finely divided cobalt hydroxide–lithium hydroxide mixtures, obtained by precipitation (2). Amatucci *et al.* prepared HT-$LiCoO_2$ powders at temperature as low as 100°C through the use of a two-day ion exchange reaction between CoOOH and an excess of $LiOH \cdot H_2O$ in the presence of a small amount of added water as well as in autoclave (3). The product had some amounts of carbonate and hydroxyl species. By heating at moderate temperatures, around 250°C, the authors succeeded in removing these species and improving the electrochemical cycling properties.

Among other promising low-temperature techniques is mechanical activation (MA). This technique makes it possible to obtain highly dispersed and disordered compounds at nearly room temperature. Fernandez-Rodriguez *et al.* found that $LiCoO_2$ was formed after extensive grinding (40 h) of a mixture of $LiOH \cdot H_2O$ and $Co(OH)_2$ in agate milling jars in air (8). However, they experienced some difficulties due to the partial decomposition of $LiCoO_2$ with the formation of Co_3O_4. Obrovac *et al.* tried to obtain disordered $LiCoO_2$ with improved electrochemical performance by MA, but failed due to the noticeable instability of $LiCoO_2$ under mechanical loading (9). In both studies the researchers obtained disordered and nonhomogeneous $LiCoO_2$. The authors claimed that the sample phase nonhomogeneity was the main reason for the degradation of their electrochemical performance. However, the change in the electronic state of cobalt ions in MA-$LiCoO_2$ was not investigated.

In the present study we tried to determine whether the MA method is suitable for providing a disordered but homogeneous $LiCoO_2$ with therefore a more effective electron correlation of cobalt ions. $LiCoO_2$ samples were prepared both by MA of the mixtures of various initial reagents (“reactive grinding”) and by MA of ceramically prepared $LiCoO_2$ (“nonreactive grinding”). The main goal of this study was to determine whether a relation between the structural parameters and the electronic state of cobalt ions in mechanochemically prepared $LiCoO_2$, as well as its electrochemical performance as cathode material, does exists.

EXPERIMENTAL

LiOH (Aldrich), CoOOH, $Co(OH)_2$ (UM Belgium), and Co (polyol) were used as initial reagents. CoOOH was prepared by oxidation of $Co(OH)_2$ using 8 M NaClO as oxidizing agent in the present of 5 M KOH (10). Ceramic $LiCoO_2$ was synthesized from a stoichiometric mixture of Li_2O and Co_3O_4 heat treated at 900°C.

Mechanical activation was carried out in a Spex 8000 mixer mill that generates normal mechanical strain, using stainless jars and balls. The mass ratio of material to balls was 1/20. Grinding time varied from 1 to 10 h. MA was performed in air or oxygen. The stoichiometric Li/Co molar ratio was used in the starting mixtures. The activated samples were then heated at 400°C for 4 h in air. Ceramic HT-$LiCoO_2$ was ground under similar milling conditions.

The final products were characterized by X-ray diffraction using a Scintag diffractometer with CuK_α radiation (1.5418 Å). IR spectra were recorded on a Bruker FTIR spectrometer using CsI pellets. Thermal analysis was performed in air with a Setaram TG-DTA 92 apparatus using alumina crucibles. The rate of heating was 10°C/min. Diffuse reflectance electron spectra (DRS) were recorded using a Shimadzu spectrophotometer in the range 11,000–50,000 cm^{-1}. A Scanning Philips field effect gun (FEG) XL-30 electron microscope (SEM) with a resolution of about 1 nm was used to study morphology changes. Electrochemical tests were carried out in a galvanostatic mode with a C/10 charge/discharge rate, using a MacPile system (Biologic S.A., Claix, France).

RESULTS AND DISCUSSION

Table 1 displays the results of the thermodynamic estimation of $\Delta G^0_{298\ K}$ for the reactions of $LiCoO_2$ formation from LiOH and cobalt compounds exhibiting various oxidation states of cobalt ions. It shows that at room temperature the reaction with metallic cobalt is thermodynamically more feasible. As the cobalt oxidation state of the initial precursors increases, the $\Delta G^0_{298\ K}$ value becomes more positive. Note that only reaction (1) occurs in the absence of oxygen. When using metallic cobalt or $Co(OH)_2$, $LiCoO_2$ synthesis proceeds through an oxidation

TABLE 1
ΔG^0_{298} for Reactions of the $LiCoO_2$ Formation[a]

	Reaction	Co oxidation state	ΔG kJ/mol $LiCoO_2$
1	$LiOH + CoOOH \rightarrow LiCoO_2 + H_2O$	+3	−31.3
2	$LiOH + 1/3Co_3O_4 + 1/12O_2 \rightarrow LiCoO_2 + 1/2H_2O$	+2, +3	−34.1
3	$LiOH + Co(OH)_2 + 1/4O_2 \rightarrow LiCoO_2 + 3/2H_2O$	+2	−105.1
4	$LiOH + Co + 3/4O_2 \rightarrow LiCoO_2 + 1/2H_2O$	0	−281.9

[a] $\Delta G^0_{f,298}$ of compounds being used: $-619.\sigma$kJ/mol for $LiCoO_2$ (11); −455.6 kJ/mol for LiOH (12); −413.8 kJ/mol for $Co(OH)_2$ (13); $-744.\sigma$ kJ/mol for Co_3O_4 (13); −369.1 kJ/mol for CoOOH (14)

of Co or Co^{2+} to Co^{3+}, while using CoOOH such oxidation is not necessary, except that the dehydration of CoOOH with the formation of Co_3O_4 does take place.

1. Reactive Grinding

TG-DTA data highlight an appreciable difference in the thermal behavior of the activated and nonactivated mixtures. The heating of the nonactivated LiOH + CoOOH mixture is accompanied by three endothermic effects at 50–150, 320–330, and 450°C (Fig. 1a). They were assigned (i) to the adsorbed water removal from LiOH in the course of the sample preparation, and (ii) to the processes of CoOOH decomposition and (iii) of LiOH melting, respectively. All effects are coupled with the corresponding mass loss. In contrast, the DTA curve for activated mixture is quite less busy with the presence of a single endothermic peak at 50–200°C, associated with the elimination of gaseous products. Surprisingly, the interaction with the $LiCoO_2$ formation was not found to occur with a noticeable thermal effect in both cases. This phenomenon contrasts with the exothermic effect observed at 380°C by Antolini when heating a mixture of Li_2CO_3 with Co_3O_4, and interpreted as a $LiCoO_2$ formation (15).

Similar differences were observed for the initial and the activated LiOH + $Co(OH)_2$ mixtures. The DTA heating curve of the initial mixture is characterized by two endothermic peaks in the low-temperature region (below 300°C) and one endothermic at 400–500°C. Both peaks showing at low and high temperature have the same origin as those mentioned above while the middle one is associated with the dehydration of initial cobalt hydroxide into Co_3O_4 as deduced by a separate X-ray study (8). Such differences disappear after MA; the DTA line for the latter sample is close to that observed for the activated LiOH + CoOOH mixture.

As shown in Fig. 1b, the heating of the nonactivated LiOH + Co mixture is accompanied by an endothermic peak at 100°C and an intense exothermic one at 380–480°C, associated with the elimination of adsorbed water and the metallic cobalt oxidation concomitant with the $LiCoO_2$ formation, respectively. For the activated mixture, both peaks are still present with, however, an increase in intensity for the first one and a decrease for the second, with the latter becoming wider (350–550°C).

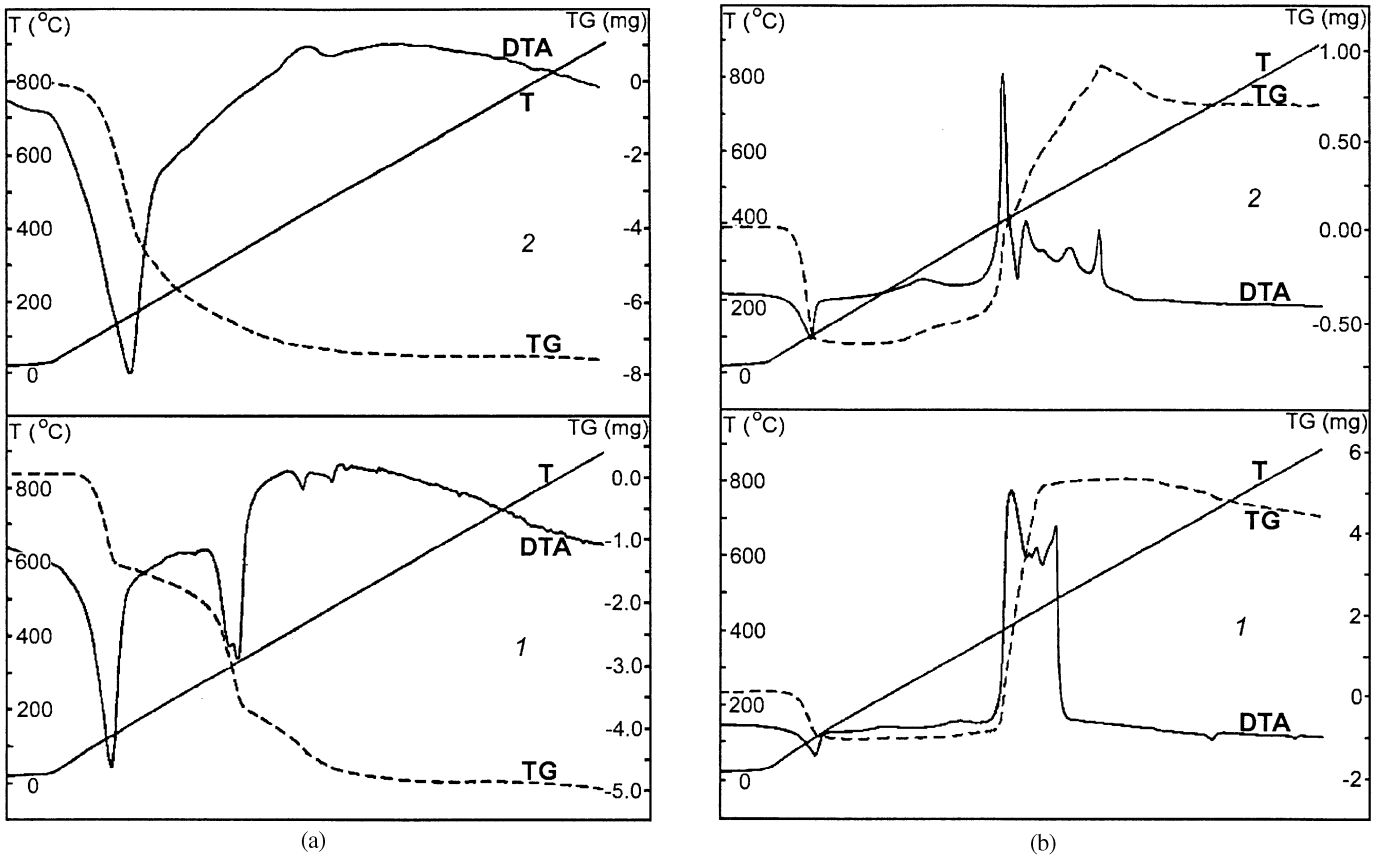

FIG. 1. TG and DTA curves of initial (1) and ground (2) mixtures: LiOH + CoOOH (a) and LiOH + Co (b).

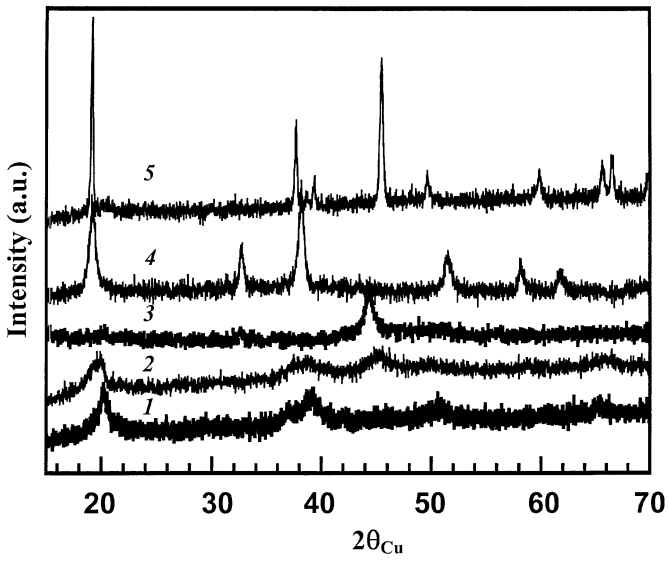

FIG. 2. X-ray patterns of ground samples (1 h): CoOOH (1); LiOH + CoOOH (2); LiOH + Co (3); LiOH + $Co(OH)_2$ (4); LiOH + CoOOH ground and heated at 600°C (5).

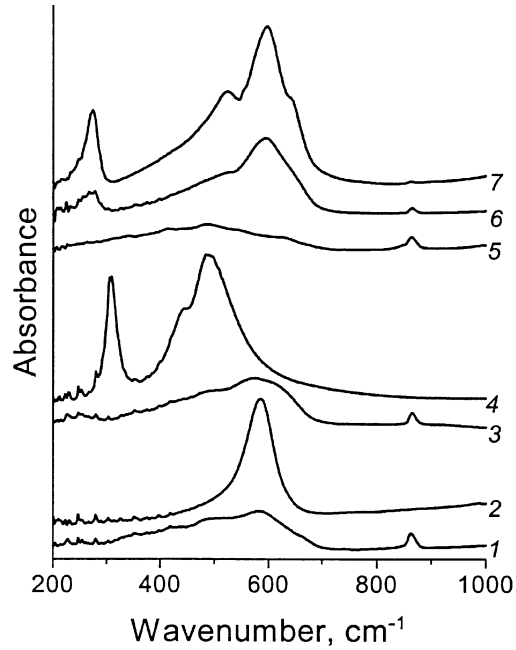

FIG. 3. FTIR spectra of ground samples (1 h); LiOH + CoOOH (1); LiOH + $Co(OH)_2$ (3); LiOH + Co (5); $LiCoO_2$ (6) and initial compounds CoOOH (2); $Co(OH)_2$ (4); $LiCoO_2$ (7).

X-ray diffraction patterns of the mixtures of LiOH with CoOOH, $Co(OH)_2$, and Co, ground for 1 h in air, are shown in Fig. 2. The reflections of LiOH are absent in all the patterns due to the hydroxide amorphization and a weak scattering of lithium atoms. For the LiOH + Co (curve 3) and LiOH + $Co(OH)_2$ (curve 4) mixtures, the X-ray patterns of the ground samples exhibit characteristics similar to those of the individual Co and $Co(OH)_2$, respectively, with however wider and less intensive reflections due to the amorphization of the starting compounds upon grinding. In addition, color changes are observed as the pink initial $Co(OH)_2$-based mixture turns brown due to a partial oxidation of the cobalt hydroxide.

The ground LiOH + CoOOH mixture exhibits a poor crystallinity (Fig. 2, curve 2). However, four main broad X-ray peaks can be distinguished. A new broad peak in the 44–48° 2θ range appears, which does not exist in the ground CoOOH (curve 1). Based on the crystallographic data of LT-$LiCoO_2$ reported in the literature (see above), we can conclude that LT-$LiCoO_2$ is formed upon MA of the LiOH + CoOOH mixture. Note that You *et al.* have recently reported the formation of LT-$LiCoO_2$ by grinding the stoichiometric Li_2O_2 + Co mixture for 10 h (16).

Since crystallinity of the ground samples is rather poor, the X-ray diffraction technique provides limited information and needs to be completed by other methods. The local environment of the cations against neighboring oxygen atoms has been determined by infrared spectroscopy.

Figure 3 shows FTIR spectra of as-prepared $LiCoO_2$ as well as of the ceramic one before and after grinding in comparison with the initial compounds. The spectra of CoOOH (curve 2) and $Co(OH)_2$ (curve 4) are described by intense bands in the 500–650 and 300–600 cm^{-1} ranges, respectively. The IR characterization of ceramic layered $LiCoO_2$ is well described in the literature (17). Briefly, based on the factor group analysis of D^5_{3d}, four IR active modes ($2A_{2u} + 2E_u$) distributed over two different frequency regions are present. The bands of the CoO_6 vibrations are within the range 400–650 cm^{-1}, while the LiO_6 vibrations are within the range 200–400 cm^{-1}. The FTIR spectrum of ceramic $LiCoO_2$ (curve 7) matches well the existing literature data through the presence of one band at 270 cm^{-1}, corresponding to the Li–O vibration, and a larger one centered at 600 cm^{-1}, corresponding to the Co–O vibration.

Noticeable change in the spectra of all ground samples are observed. Whatever the starting compounds, the bands become broader and less intense after 1 h of MA, most likely resulting from sample amorphization and a decrease in particle size. A broad band in the range 450–600 cm^{-1} appears in the spectrum of the activated LiOH + CoOOH mixture, instead of a single band at 595 cm^{-1} in the spectrum of the initial CoOOH, indicating the early stage of the $LiCoO_2$ formation (Fig. 3 curve 1). In the spectrum of the LiOH + $Co(OH)_2$ mixture (curve 3), a sharp decrease in the band intensity, corresponding to initial $Co(OH)_2$, is observed. In addition, one can see a new broadband appearing at 500–700 cm^{-1}. A sharp decrease in band

intensity and the appearance of continuous absorption of the LiOH + Co mixture (curve 5) suggest the presence of a large amount of conductive electrons in the system.

In the range 1000 to 4000 cm^{-1} (not reported here) all spectra of activated mixtures indicate the presence of CO_3^{2-} and proton-containing groups with strong hydrogen bonds. It is well known that MA increases the sensitivity of oxides to the ambient atmosphere.

Overall, the IR study leads to the conclusion that for both precursors, $Co(OH)_2$ and CoOOH, the environment of cobalt ions in the activated mixtures is altered due to the formation of poor crystallized $LiCoO_2$.

SEM micrographs (Fig. 4a) show the appearance of mechanically driven layered dense composites in the activated mixture of lithium and cobalt hydroxides instead of plate-like hexagonal particles characteristic of cobalt hydroxides. Surprisingly, the metallic cobalt spherical particles were not significantly destroyed under MA in the mixtures with LiOH (Fig. 4b), in contrast to their full distortion observed when activated alone. In our opinion, this is due to the layered structure of LiOH and its good plasticity, preventing the process of strong distortion of metallic particles.

Thus, MA of the mixtures under study brings about different results, depending on the nature of the reagents used. When using metallic cobalt, an intimate mixing of reagents occurs, accompanied by the hardly noticeable oxidation process of Co^0. Partial oxidation of $Co(OH)_2$ is observed for the $Co(OH)_2$-based mixture, whereas the LT-$LiCoO_2$ formation occurs in the CoOOH-based mixture. Considering thermodynamic data (Table 1), this result indicates that the formation of $LiCoO_2$ from $Co(OH)_2$ and Co are hampered, probably due either to a lack of sufficient amount of oxygen in the jars or to the reaction of the Co^{2+} ions oxidation being a diffusion-controlled one. Special experiments, performed with the LiOH + Co mixture in an oxygen atmosphere (20 atm), did not show a noticeable influence of gas atmosphere on the mechanochemical synthesis of $LiCoO_2$, suggesting a more complex reacting mechanism to be identified.

2. Thermal Treatment of Activated Samples

All activated mixtures were heat treated at 600°C for 4 h in air. Whatever the precursors, the obtained heat-treated compounds exhibited X-ray patterns similar to that of layered HT-$LiCoO_2$ (Fig. 2, curve 5). Therefore, the spinel-frame LT-$LiCoO_2$, formed from the activated LiOH + CoOOH mixture, was changed into a hexagonal HT-$LiCoO_2$ phase upon heating. The formation of HT-$LiCoO_2$ after heat treatment of the activated mixture was confirmed by IR spectroscopy (spectra not shown here).

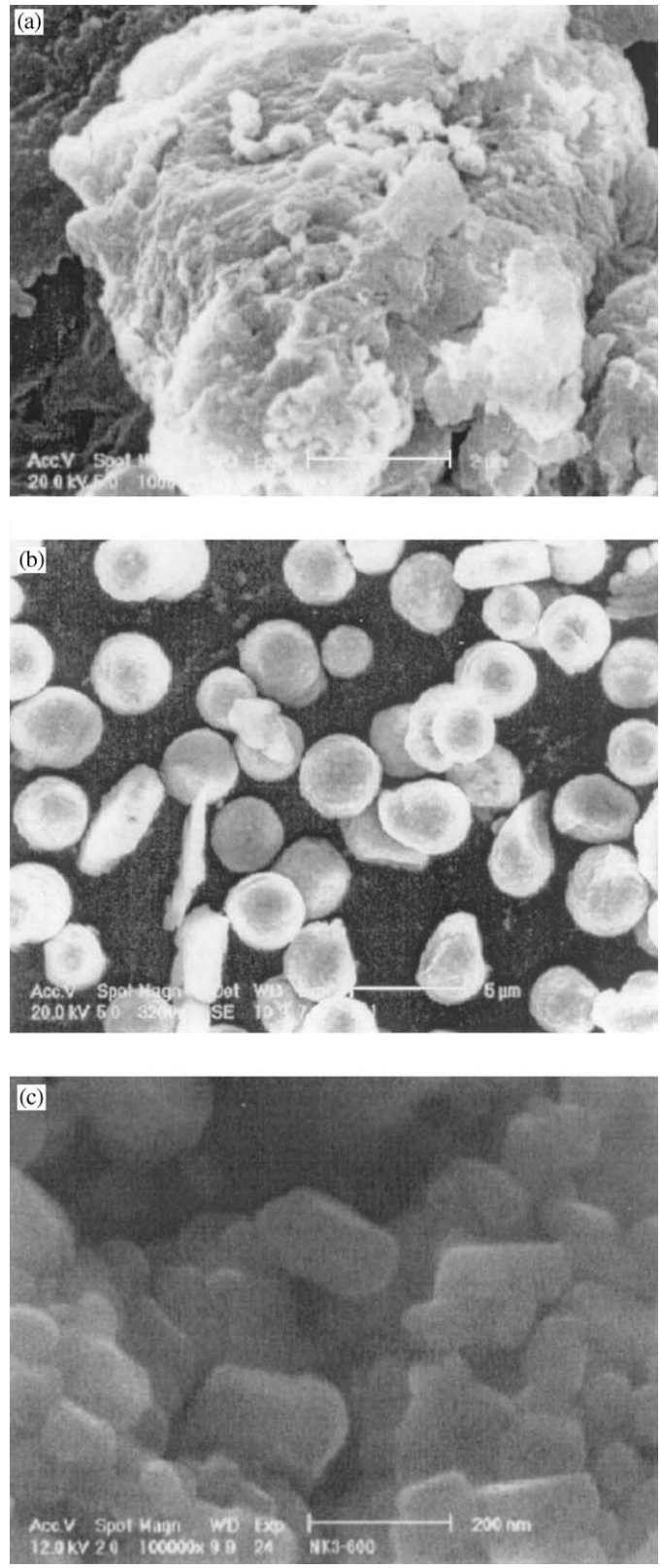

FIG. 4. SEM micrographs of ground samples (1 h): LiOH + CoOOH (a); LiOH + Co (b); LiOH + CoOOH ground and heated at 600°C (c).

According to electron microscopy data, the heated samples consists of small spherical particles having an average size of 100–200 Å (Fig. 4c).

3. Nonreactive Grinding

In parallel to the reactive grinding experiments described above, a study dealing with the nonreactive grinding of ceramic HT-$LiCoO_2$ was also carried out. The evolution of the X-ray patterns with grinding time is shown in Fig. 5. The X-ray line broadening suggests a sample amorphization coupled with a reduction in particle size upon grinding. We did not observe an inversion of the relative intensities of the 003 and 104 reflections as reported by Fernandez-Rodriguez *et al.* (8). The full destruction of the layered structure (i.e., disappearance of the 003 peak) was observed only after 10 h of grinding. The X-ray pattern of the sample ground for 10 h exhibits three main peaks (marked with *) corresponding to a phase that can be indexed in a cubic symmetry and whose exact stoichiometry is unknown. Upon grinding ceramic $LiCoO_2$, the IR study, showing the appearance of bands characteristic of the compound Li_2CO_3 (spectra not given here), suggests a delithiation of $LiCoO_2$ while the broadening of the Co–O bands in the region 400–700 cm^{-1} (Fig. 3, curve 6) indicates a decreases in sample homogeneity.

4. Electronic State of Cobalt Ions in as Prepared $LiCoO_2$ Samples

The electronic state of Co ions in the as-prepared samples was investigated by diffuse reflectance electron spectroscopy (DRS). Spectra interpretation based on the analysis of the peculiarities of Co^{2+} or Co^{3+} ion absorption bands versus the oxygen crystal field (18,19) was performed.

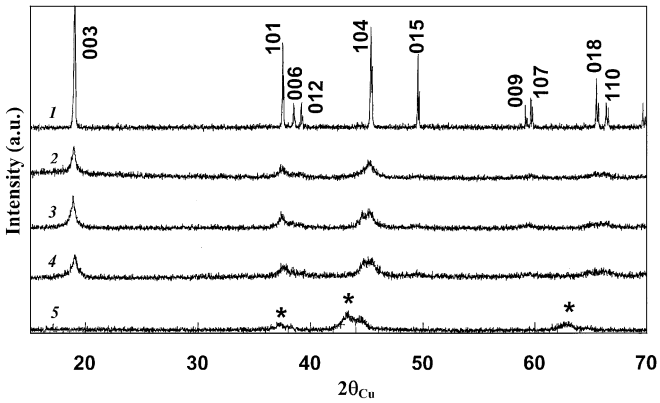

FIG. 5. X-ray pattern of ceramic $LiCoO_2$ as-prepared (1) and ground for 1 (2), 3 (3), 5 (4), and 10 h (5). * corresponds to a new phase indexed in a cubic symmetry.

(a) Co^{2+} ions in octahedral oxygen crystal field—$[Co^{2+}]_{Oh}$. The ^4F term is the ground atom term for a free Co^{2+} ion (electron configuration d^7) and ^4P is the first excited term. According to Tanabe–Sugano diagrams, for the oxygen octahedral complexes of high-spin Co^{2+} ions, the following three transitions from the ground state $^4T_{1g}$ are possible: $^4T_{1g}$–$^4T_{2g}$ (ν_1) $^4T_{1g}$ –$^4A_{2g}$ (ν_2), $^4T_{1g}$(F) –$^4T_{1g}$(P) (ν_3). The energy of the ν_1 transition is usually small (less than 10,000 cm^{-1}). The ν_2 transition is a two-electron transition and therefore characterized by a small extinction (intensity). Thus, for this case, the ν_3 transition is more likely to occur. It can be displayed by a multiple structure or a broadening of the spectrum due to an admixing of the excited states. The analysis of literature data shows that for Co^{2+} ions, stabilized in perfect oxygen octahedral coordination, for example, in solid $Co_3Si_4(OH)_2 \cdot nH_2O$ (20), the ν_3 transition is observed in the region 19,000–20,000 cm^{-1}, thus, being a good signature of these ions. Let's just remember the low intensity of the transition for perfect structures. However, a structural disordering (i.e., the presence of structural defects) or a cation–cation magnetic exchange interaction enhances the transition intensity.

(b) Co^{2+} ions in tetrahedral oxygen crystal field—$[Co^{2+}]_{Td}$. For high-spin Co^{2+} ions in a tetrahedral coordination, three types of transitions from the ground state $^4A_{2g}$ are also possible: $^4A_{2g}$–$^4T_{2g}$ (ν_1), $^4A_{2g}$–$^4T_{1g}$ (ν_2), $^4A_{2g}$(F) –$^4T_{1g}$(P) (ν_3). For oxygen ligands, the ν_1 and ν_2 transitions appear in the low-frequency region (less than 10,000 cm^{-1}). A good example of Co^{2+} ions in a tetrahedral crystal field is $CoCr_2O_4$. For solid $CoCr_2O_4$, the ν_3 transition is observed at 15,000–17,000 cm^{-1} (20). It is well known (18) that the extinction of all transitions for $[Co^{2+}]_{Td}$ is significantly higher than for $[Co^{2+}]_{Oh}$, making it easy to distinguish this cobalt state along with $[Co^{2+}]_{Oh}$ even if it is present in small amounts.

(c) Co^{3+} ions in octahedral oxygen crystal field—$[Co^{3+}]_{Oh}$. For free Co^{3+} ion (electron configuration d^6) ^5D appears to be the atom ground term. For oxygen ligands, a low-spin state with the lowest $^1A_{1g}$ state is usually reported (21). In this case the following transitions are possible: $^1A_{1g}$–$^3T_{1g}$ (ν_1), $^1A_{1g}$–$^1T_{2g}$ (ν_2), $^1A_{1g}$–$^1T_{1g}$ (ν_3), and $^1A_{1g}$–$^1T_{2g}$ (ν_4). Two transitions with the energy of about 16,000–17,000 cm^{-1} (ν_3) and 22,000–24,000 cm^{-1} (ν_4) are characteristic of the low-spin Co^{3+} ions in octahedral coordination. Besides, *d–d* transitions from the ground to the excited state in the ultraviolet region (25,000–35,000 cm^{-1}) are also possible.

(d) Experimental spectra of CoOOH, $Co(OH)_2$, and $LiCoO_2$. In the initial $Co(OH)_2$ spectrum (space group $P\bar{3}m1$, high-spin Co^{2+} ions in Oh positions), the ν_3 transition is observed at 19,000–20,000 cm^{-1} (Fig. 6).

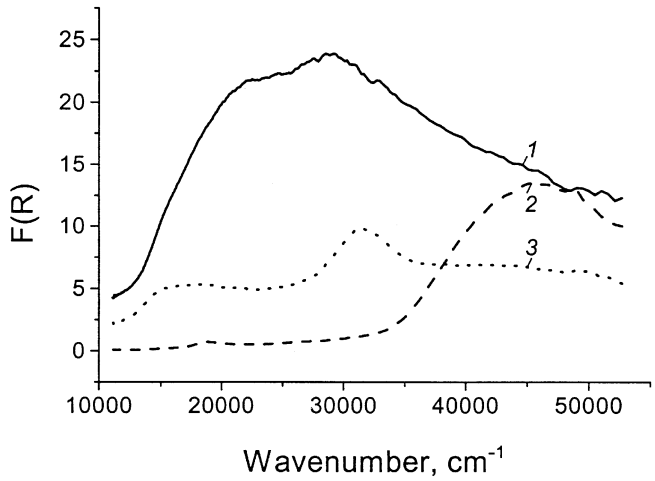

FIG. 6. DR spectra of CoOOH (1); $Co(OH)_2$ (2); and $LiCoO_2$ (3).

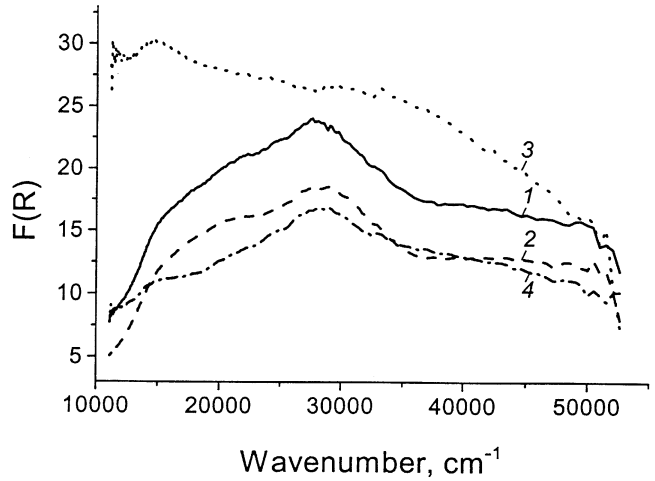

FIG. 7. DR spectra of ground samples: LiOH + CoOOH (1); LiOH + $Co(OH)_2$ (2); LiOH + Co (3); and $LiCoO_2$ (4).

Moreover, a strong band in the ultraviolet region ($>32{,}000\,cm^{-1}$) is present, which, to our opinion, is associated with a ligand–metal charge transfer (CT). The shape of the observed spectrum together with its low intensity are indicative of a high degree of homogeneity of an octahedral environment of Co^{2+} ions in the sample.

In CoOOH (space group $R\bar{3}m$, Co^{3+} ions in Oh positions), the majority of cobalt ions are low-spin Co^{3+} ions with two different types of an oxygen octahedron environment as the appearance of two bands at 27,000 and $22{,}000\,cm^{-1}$ suggests (Fig. 6, curve 1). The former is associated with a more perfect octahedron while the latter with a less perfect one, composed of O^{2-} ions and OH groups. The band at $22{,}000\,cm^{-1}$ unlikely corresponds to $[Co^{2+}]_{Oh}$. Small traces of $[Co^{2+}]_{Td}$ ($15{,}000\,cm^{-1}$) are also observed, probably due to the presence of Co_3O_4 as an admixture.

The spectrum of ceramic $LiCoO_2$ (space group $R\bar{3}m$, Co^{3+} ions in Oh positions) is characterized by a comparatively low intensity, the same as for $Co(OH)_2$ (Fig. 6, curve 3). The absorption takes place in two regions: in the low-frequency region ($13{,}000$–$20{,}000\,cm^{-1}$) and in an ultraviolet region ($28{,}000$–$35{,}000\,cm^{-1}$). The bands at $18{,}000$–$19{,}000\,cm^{-1}$ and $15{,}000\,cm^{-1}$ are associated with the ν_3 transition of $[Co^{2+}]_{Oh}$ $[Co^{2+}]_{Td}$ ions, respectively. The latter (at $28{,}000$–$35{,}000\,cm^{-1}$) is a characteristic of $[Co^{3+}]_{Oh}$ in a highly perfect octahedral environment. Hereby, the ceramic $LiCoO_2$ is characterized by small amounts of Co^{2+} ions in its structure and Co_3O_4 as an admixture.

Thus, DRS can provide qualitative information on the electronic state of cobalt ions (valence and spin state, oxygen environment) in $LiCoO_2$ prepared by different methods. Unfortunately, it is impossible to get accurate quantitative data on the concentration of varied cobalt ions due to different extinctions of their absorption bands.

(e) Co^{3+} Co^{2+} ions in ground samples before and after heat treatment. Let's analyze the spectra of ground mixtures on the basis of the above-mentioned data. The main electronic state of cobalt ions in the LiOH + CoOOH mixture (Fig. 7, curve 1) is found to be low-spin $[Co^{3+}]_{Oh}$ ($28{,}000\,cm^{-1}$). A small amount of high-spin $[Co^{2+}]_{Td}$ ions ($15{,}000\,cm^{-1}$) is also present. For the LiOH + $Co(OH)_2$ mixture, a large overall absorption is observed as compared with the initial $Co(OH)_2$, suggesting a pronounced structural disorder (Fig. 7, curve 2). Three bands located at 28,000, 18,000–19,000, and $15{,}000\,cm^{-1}$ corresponding to $[Co^{3+}]_{Oh}$, $[Co^{2+}]_{Oh}$, and $[Co^{2+}]_{Td}$ (traces) are also present. The spectrum of the LiOH + Co mixture is characterized by a large continuous absorption, probably resulting from the presence of delocalized electrons in the system (metal state) with traces of $[Co^{2+}]_{Td}$, which are badly noticeable in the background (Fig. 7, curve 3). In the spectrum of the activated $LiCoO_2$, a more intense band belonging to $[Co^{3+}]_{Oh}$ is significantly shifted to a low-frequency region as compared with nonactivated $LiCoO_2$. This phenomenon may be explained by a weakening of the crystal field effect as a result of the distortion of the anionic framework by residual OH^- Co_3^{2-} groups. Moreover, the bands corresponding to $[Co^{2+}]_{Td}$ and $[Co^{2+}]_{Oh}$ increase in intensity.

The DR spectra of all ground mixtures heated at 600°C become similar (Fig. 8). The main state of the cobalt is $[Co^{3+}]_{Oh}$, with a localization in a more perfect oxygen crystal field ($32{,}000$–$33{,}000\,cm^{-1}$) as compared with those without heating. However, the observed shift of the right edge of this band to a high-frequency UV region indicates

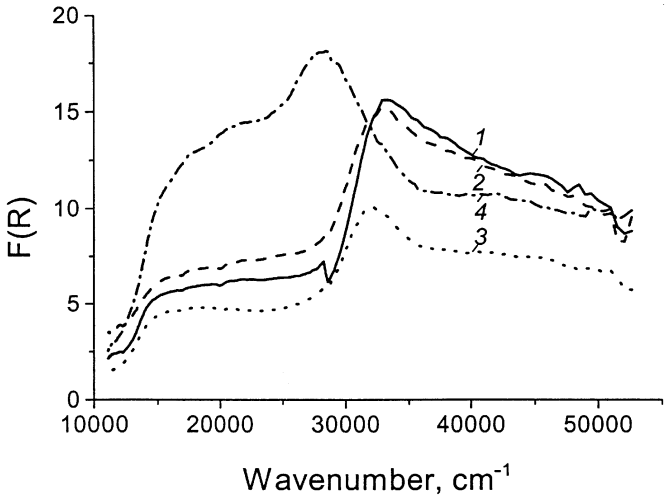

FIG. 8. DR spectra of ground samples after heating at 600°C: LiOH + CoOOH (1); LiOH + $Co(OH)_2$ (2); LiOH + Co (3); and $LiCoO_2$ (4).

probably crystal field inhomogeneity around Co^{3+} ions (oxygen defects) or the formation of Co^{3+} ions' clusters. It should be noted that heating the LiOH + Co mixture leads to the full oxidation of cobalt ions localized in more homogeneous $Co^{3+}O_6$ octahedra. The lower intensity of the 15,000 cm^{-1} band most likely corresponds, as mentioned above, to the *d–d* transition of high-spin Co^{2+} ions in Co_3O_4 (admixture). In contrast, the heating of the activated ceramic $LiCoO_2$ does not lead to significant improvements of Co^{3+} octahedra; the band at 28,000–29,000 cm^{-1} is still observed.

Thus, according to DRS study, the ground mixtures are characterized by strong nonhomogeneity in the electronic state of cobalt ions as well as their various oxygen environments. The annealing of the samples results in an enhancement of the Co^{3+} homogeneity. All spectra of the annealed samples are characterized by localized states only (i.e., ions). No delocalized electrons were detected in the structure of as-prepared $LiCoO_2$ samples.

5. *Electrochemical Performance of As-Prepared $LiCoO_2$ Samples*

The voltage–composition curves of the $LiCoO_2$//Li cells made with the ground LiOH + CoOOH mixture, which is believed to correspond to LT-$LiCoO_2$, are shown in Fig. 9. The very large capacity of 0.7 Li observed upon the first charge is followed by a first discharge of 0.1 Li, indicating a very poor reversibility of the system. The large capacity of the first charge may be attributed to the reactivity of adsorbed impurities versus lithium or electrolyte.

The heating of the ground samples at 600°C resulting in the formation of HT-$LiCoO_2$ leads to a strong improvement of the cycling properties. The voltage–composition

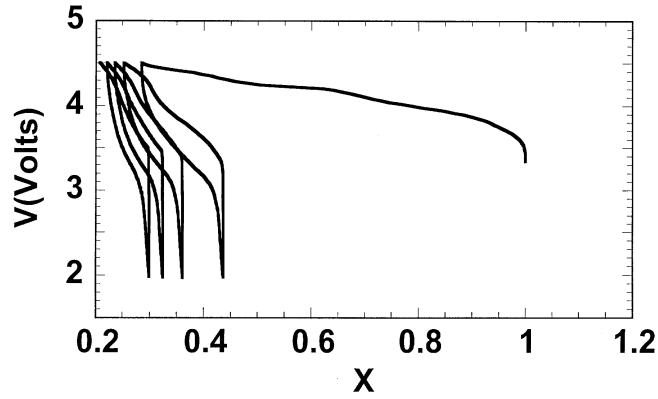

FIG. 9. Charge–discharge curve of ground sample LiOH + CoOOH.

curve of $LiCoO_2$/Li cells made with the ground LiOH + Co mixture heat treated at 600°C is shown in Fig. 10. The cell behavior is similar to that usually observed for layered HT-$LiCoO_2$. A reversible capacity of 0.35 Li is obtained with, however, a noticeable irreversibility at the first cycle. This sample was shown by DRS to present a better electron homogeneity of Co^{3+} ions.

CONCLUSION

It has been demonstrated that a short mechanical activation combined with a subsequent annealing at moderate temperatures enables the formation of disordered, highly dispersed, and rather homogeneous $LiCoO_2$ samples. The main electronic state of cobalt ions in as-prepared $LiCoO_2$ is a low-spin $[Co^{3+}]_{Oh}$ with some oxygen crystal field nonhomogeneity, probably due to the forma-

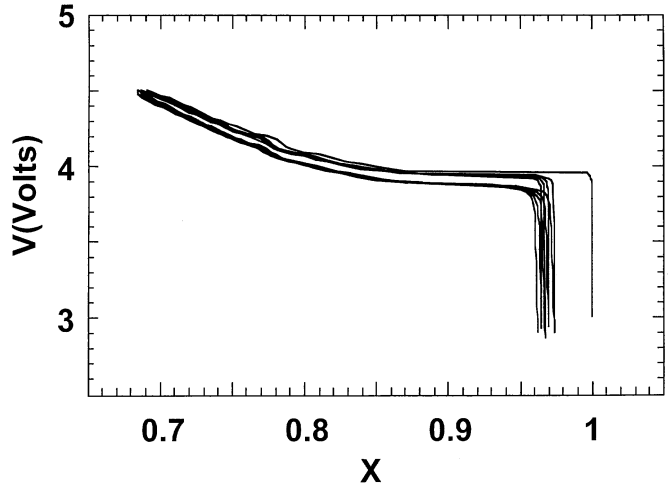

FIG. 10. Charge–discharge curve of ground sample LiOH + CoOOH after heating at 600°C.

tion of oxygen defects. Using the DRS technique, traces of $[Co^{2+}]_{Oh}$ ions in the structure of $LiCoO_2$ and Co_3O_4 as an admixture were detected, while they were practically undetectable by X-ray and IR spectroscopy. Furthermore, this technique has indicated that all observed *d* electrons in the as-prepared $LiCoO_2$ samples are localized. The main reason is probably the formation of definite mechanochemically induced defects (e.g., oxygen vacancies, O^- ions), which are preserved in the activated samples even after their heating at 600°C. These defects appeared to act as traps for delocalized electrons, producing cobalt ions with localized electrons. In light of these results, one can conclude that in order to prepare cathode material with enhanced electrochemical performance, it appears necessary to obtain an electronic structure placed midway between full delocalization (electron gas) and full localization (ions). Probably, this could be achieved by a fine tuning of the mechanochemical conditions and of the annealing temperature. Such electron structures were observed for Li_xCoO_2 ($x>1$) (5) as well as in our study of mechanochemically prepared LiV_3O_8 (22).

ACKNOWLEDGMENTS

The authors thank S. Langella, N. Penin, B. Roch, and S. Soiron for their fruitful discussions.

REFERENCES

1. E. Rossen, J. N. Reimers, and J.R. Dahn, *Solid State Ionics* **62,** 53 (1995).
2. Y.-M. Chiang, Y.-I. Jang, H. Wang, *et al*., *J. Electrochem. Soc*. **145,** 887 (1998).
3. G. G. Amatucci, J.-M. Tarascon, D. Larcher, and L.C. Klein, *Solid State Ionics* **84,** 169 (1996).
4. V. S. Pervov, I. A. Kedrinskii, and E. V. Mackonina, *Neorg. Mater*. **33,** 1031 (1997).
5. S. Levasseur, M. Menetrier, E. Suard, and C. Delmas, *solid State Ionics* **128,** 11 (2000).
6. N. F. Mott and E. A. Davis, "Electron Processes in Non-crystalline Materials." Clarendon Press, Oxford, 1979.
7. H. J. Orman and P. J. Wiseman, *Acta Crystallogr. C* **40,** 12 (1984).
8. J. M. Fernandez-Rodriguez, J. Morales and J. L. Tirado, *React. Solids* **4,** 163 (1987).
9. M. N. Obrovac, O. Mao, and J. R. Dahn, *Solid State Ionics* **112,** 9 (1998).
10. V. Pralong, A. Delahaye-Vidal, B. Beaudoin, *et al*., *J. Mater. Chem*. **9,** 955 (1999).
11. H. Yokokawa, N. Sakai, K. Yamaji, *et al*., *Solid State Ionics* **113,** 1 (1998).
12. O. Kubaschewskii and C. B. Alcock (Eds.), "International Series on Materials Science and Technology," Vol. 24, pp. 267–323. Metallurgical Thermochemistry, 1979.
13. R. David (Ed.), "CRC, Handbook of Chemistry and Physics." Lide, 1992.
14. R. Sonbirous, thesis. l'Universite de Paris, 1970.
15. E. Antolini, *Mater. Res. Bull*. **32**, 9 (1997).
16. H. W. You, H. Y. Lee, S. W., Jang, *et al*., *J. Mater. Sci. Lett*. **17,** 931 (1998).
17. A. Rougier, G. A. Nazri, and C. Julien, *Ionics* **3,** 170 (1997).
18. A. B. P. Lever, "Inorganic Electronic Spectroscopy." Elsevier Science, Amsterdam, 1984.
19. N. V. Kosova, V. F. Anufrienko, T. V. Larina, and E. T. Devyatkina, *Chem. Sustainable Develop*. **9,** 235 (2001). [in Russian]
20. A. A. Khassin, T. M. Yurieva, G. N. Kustova, *et al*., *Mater. Res. Innovation* **4,** 251 (2001).
21. J. S. Griffith, "The Theory of Transition-Metal Ions." Cambridge Univ. Press, Cambridge, 1961.
22. N. V. Kosova, S. V. Vosel, V. F. Anufrienko, *et al*., *J. Solid State Chem*. **160,** 444 (2001).